

Cite this: *Chem. Sci.*, 2025, 16, 7876

All publication charges for this article have been paid for by the Royal Society of Chemistry

Received 18th January 2025

Accepted 25th March 2025

DOI: 10.1039/d5sc00452g

rsc.li/chemical-science

Organocatalytic atroposelective *de novo* construction of monoaxially and 1,4-diaxially chiral fused uracils with potential antitumor activity†

Yuzhi Ren,^a Chen Lin,^a Han Zhang,^b Zuquan Liu,^a Donghui Wei,^{id}*^b Jie Feng^{id}^a and Ding Du^{id}*^a

Atropisomers bearing multiple stereogenic axes are of increasing relevance to materials science, pharmaceuticals, and catalysis. However, the catalytic enantioselective construction of these atropisomers in a single step remains synthetically challenging. We herein report the first NHC-organocatalytic enantioselective synthesis of a new class of monoaxially and 1,4-diaxially chiral fused uracil scaffolds. Preliminary studies on the antitumor activity of selected compounds demonstrated that this new class of axially chiral uracil derivatives may have potential applications in the discovery of new lead compounds in medicinal chemistry.

Atropisomers, a subtype of conformers arising from hindered rotation about a single bond, are not only widely present in natural products but also have numerous applications in medicinal chemistry, asymmetric synthesis and functional materials.¹ The past few decades have witnessed significant progress in developing effective methods for the enantioselective construction of atropisomers with a single axis.² On the other hand, the implementation of molecules with multiple stereogenic axes will lead to intriguing and more complex topological structures that may exhibit unique applications in materials science, pharmaceuticals, and catalysis. However, compared to the tremendous efforts devoted to synthesizing monoaxial atropisomers, approaches for the enantioselective construction of molecules with multiple stereogenic axes are still underdeveloped.³ In particular, the methods for constructing atropisomers with 1,4-diaxes are rather limited, due to the daunting challenge of assembling remote 1,4-diaxial systems with simultaneous enantio- and diastereocontrol. To date, the reported successful examples have mainly focused on the enantioselective synthesis of atropisomers with C–C 1,4-diaxes. In 1989, Hayashi⁴ reported the first example of the enantioselective synthesis of chiral 1,4-diaxial ternaphthalenes by Ni-catalyzed double Kumada cross-coupling of Grignard reagents with dibromonaphthalenes (Scheme 1A-1). In 2019, 30 years after Hayashi's pioneering work, Shi⁵ applied Pd-catalyzed

double Suzuki–Miyaura cross-coupling between dibromonaphthalenes and naphthylboronic acids to atroposelective synthesis of the aforementioned ternaphthalenes (Scheme 1A-1). In 2004, Shibata⁶ disclosed the second strategy for enantioselective synthesis of biaryl atropisomers with 1,4-diaxes through Ir-catalyzed [2 + 2 + 2] cycloaddition of *ortho*-substituted diaryldiynes with alkynes (Scheme 1A-2). Shortly after that, Tanaka's group⁷ developed a similar stereoselective [2 + 2 + 2] cycloaddition of diketodiyne and monoalkynes, delivering anthraquinones with stereogenic 1,4-diaxes. Recently, Shibata reported a Rh-catalyzed cycloisomerization strategy closely related to [2 + 2 + 2] cycloaddition for atroposelective synthesis of 1,4-diaxially chiral polycyclic hydrocarbons.⁸ In 2018, Yan⁹ reported a new strategy for the construction of enantioenriched axially chiral 1,4-distyrene 2,3-naphthalene diols through an organocatalytic nucleophilic addition of sulfones to *in situ* generated vinylidene *o*-quinone methides (Scheme 1A-3). In 2020, Miller and Toste¹⁰ demonstrated an elegant strategy for synthesizing 1,4-biaxial terphenyl atropisomers *via* two consecutive distinct dynamic kinetic resolutions (Scheme 1A-4). During the preparation of our manuscript, Cai¹¹ reported an enantioselective synthesis of naphthalenes with 1,3,4-triaxes *via* a sequential Diels–Alder reaction and dehydrative aromatization. Despite these achievements, the enantioselective synthesis of 1,4-diaxial atropisomers is still in its infancy, and the pursuit of rapid and efficient methods to obtain structurally diverse atropisomers with different 1,4-diaxes in a single step is in high demand but remains challenging.

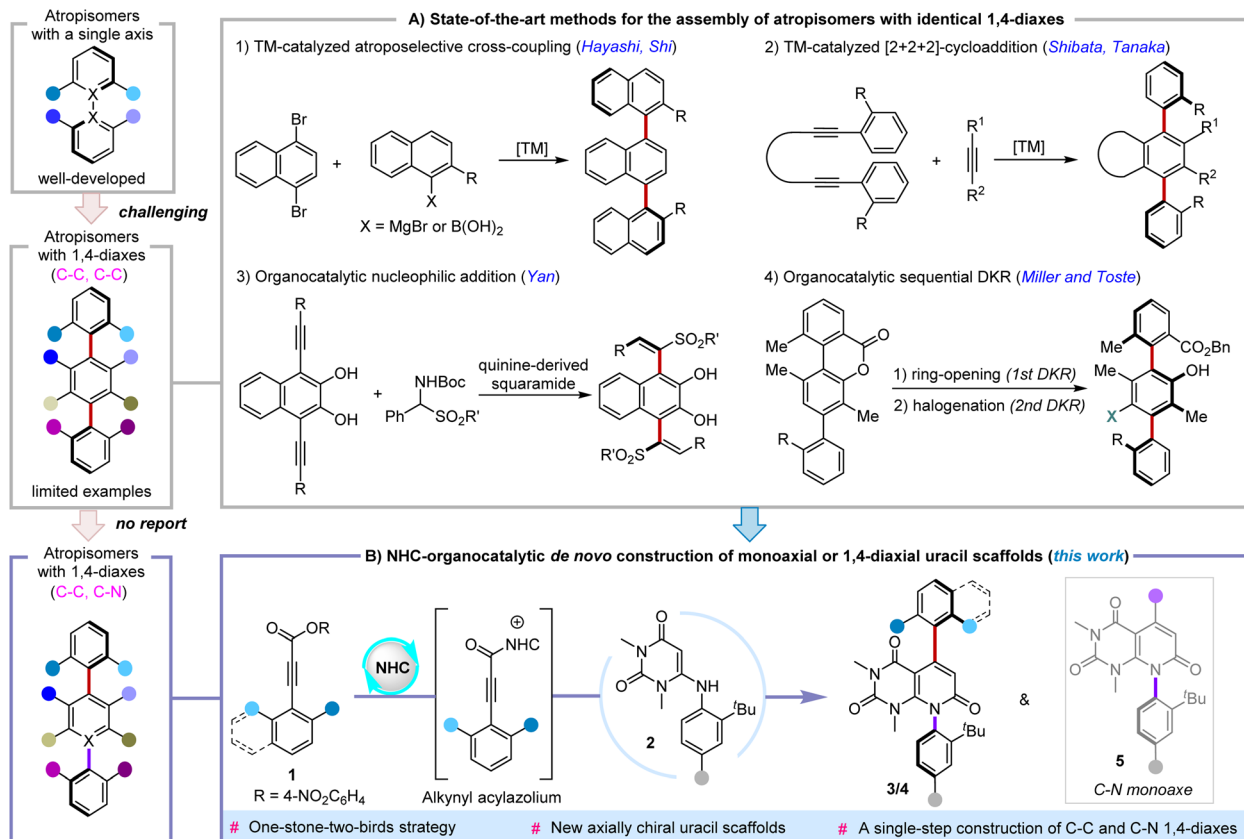
Over the past few decades, N-heterocyclic carbenes (NHCs) have provided a diverse range of unique reactive intermediates and reaction modes, enabling the acquisition of various functional molecules, especially those with central chirality.¹² The

^aSchool of Science, China Pharmaceutical University, Nanjing, 210009, P. R. China. E-mail: ddmn9999@cpu.edu.cn

^bCollege of Chemistry, Zhengzhou University, Zhengzhou, Henan Province, 450001, P. R. China. E-mail: donghuiwei@zzu.edu.cn

† Electronic supplementary information (ESI) available. CCDC 2412375 and 2412377. For ESI and crystallographic data in CIF or other electronic format see DOI: <https://doi.org/10.1039/d5sc00452g>





Scheme 1 Methods for the assembly of atropisomers with stereogenic 1,4-diaxes.

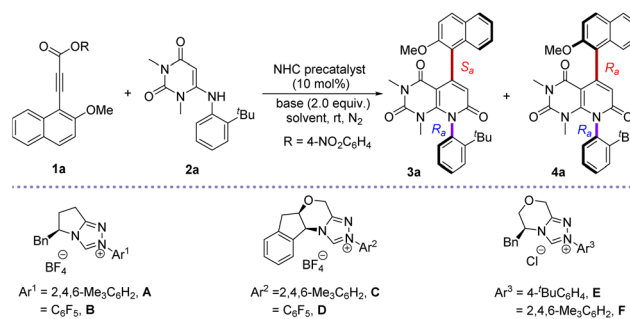
application of NHC catalysis as an effective tool for constructing axially chiral molecules has emerged as a growing area in recent years.¹³ However, the reported strategies typically involve constructing diverse atropisomers with a single axis. The enantioselective construction of atropisomers with multiple stereogenic axes is still challenging and very limited.¹⁴ To the best of our knowledge, atropisomers exhibiting C-C and C-N 1,4-diaxial chirality have not been disclosed yet. To address this synthetic challenge, we aimed to design a step-economic and stereoselective protocol that focused on NHC-catalyzed atroposelective *de novo* construction of novel heterocyclic frameworks featuring C-C and C-N 1,4-diaxes. Herein, we wish to report a single-step *de novo* construction of a new class of fused uracil scaffolds (pyrido[2,3-*d*]pyrimidines) **3/4** with C-C and C-N 1,4-diaxes through NHC-catalyzed atroposelective formal (3 + 3) annulation of 2,6-disubstituted alkyne esters **1** and 6-amino-uracils **2** (Scheme 1B) *via* alkynyl acylazolium intermediates.¹⁵ This protocol also features a one-stone-two-birds strategy for highly enantioselective synthesis of fused uracil atropisomers **5** with a C-N single axis.

We started our study by using 3-(2-methoxynaphthalene-1-yl) propionate **1a** and 6-(2-*tert*-butylphenyl)aminouracil **2a** as the model substrates for reaction condition optimization, to test the feasibility of constructing a fused uracil framework bearing stereogenic C-C and C-N 1,4-diaxes (Table 1). Initially, an array of NHC precursors (**A-F**) were used to promote the reaction

using Et₃N as a base in DMF at room temperature (entries 1–6). As a result, the reaction in the presence of precatalysts **A** and **C-F** proceeded smoothly to afford the desired diastereomers **3a/4a** with stereogenic 1,4-diaxes. **F** was found to be the optimal catalyst, in the presence of which diastereomers **3a** and **4a** were obtained in 76% combined yield with 98 : 2 er and 90 : 10 er, respectively (entry 6). Further screening of different organic and inorganic bases in the presence of catalyst **F** did not give superior results (entries 7–11). Although the results of Cs₂CO₃ were comparable to those of Et₃N, diastereoselectivity of the products and enantioselectivity of diastereomer **4a** were not improved (entry 10). Solvent screening showed that the reaction in DCM delivered the desired products with maintained enantioselectivity and better diastereoselectivity (2 : 1) albeit in a diminished yield (48%) (entry 12). Therefore, DMF and DCM were used as a combined solvent in an attempt to improve both diastereoselectivity and enantioselectivity of the reaction (entries 16–17). It was found that when DCM and DMF (2 : 1) were used as the solvent, the reaction gave diastereoisomers **3a** and **4a** in a 65% combined yield, both of which exhibited excellent enantioselectivity (98 : 2 er), although the diastereoselectivity was not improved. Finally, the conditions shown in entry 17 were established as the optimal ones for further substrate scope exploration.

With the optimized conditions in hand, the reaction scope for the synthesis of fused uracils **3/4** bearing 1,4-diaxes was then



Table 1 Optimization of the reaction conditions^a

Entry	NHC	Base	Solvent	Yield ^b (%)	dr ^c , er ^d
1	A	Et ₃ N	DMF	71	1.4 : 1, 94 : 6/51 : 49
2	B	Et ₃ N	DMF	0	—
3	C	Et ₃ N	DMF	77	1 : 1, 83 : 17/70 : 30
4	D	Et ₃ N	DMF	78	1 : 1, 76 : 24/65 : 35
5	E	Et ₃ N	DMF	73	1 : 1.5, 80 : 20/80 : 20
6	F	Et ₃ N	DMF	76	1 : 1.3, 98 : 2/90 : 10
7	F	DIPEA	DMF	72	1 : 1, 98 : 2/85 : 15
8	F	DABCO	DMF	42	1.5 : 1, 98 : 2/84 : 16
9	F	DBU	DMF	Trace	—
10	F	Cs ₂ CO ₃	DMF	68	1 : 1.2, 98 : 2/90 : 10
11	F	CsOAc	DMF	37	1 : 1.3, 97 : 3/89 : 11
12	F	Et ₃ N	DCM	48	2 : 1, 98 : 2/90 : 10
13	F	Et ₃ N	CHCl ₃	0	—
14	F	Et ₃ N	CH ₃ CN	<10	—
15	F	Et ₃ N	THF	<10	—
16	F	Et ₃ N	DCM : DMF (1 : 1) ^e	41	1.5 : 1, 98 : 2/98 : 2
17	F	Et ₃ N	DCM : DMF (2 : 1) ^e	65	1.5 : 1, 98 : 2/98 : 2

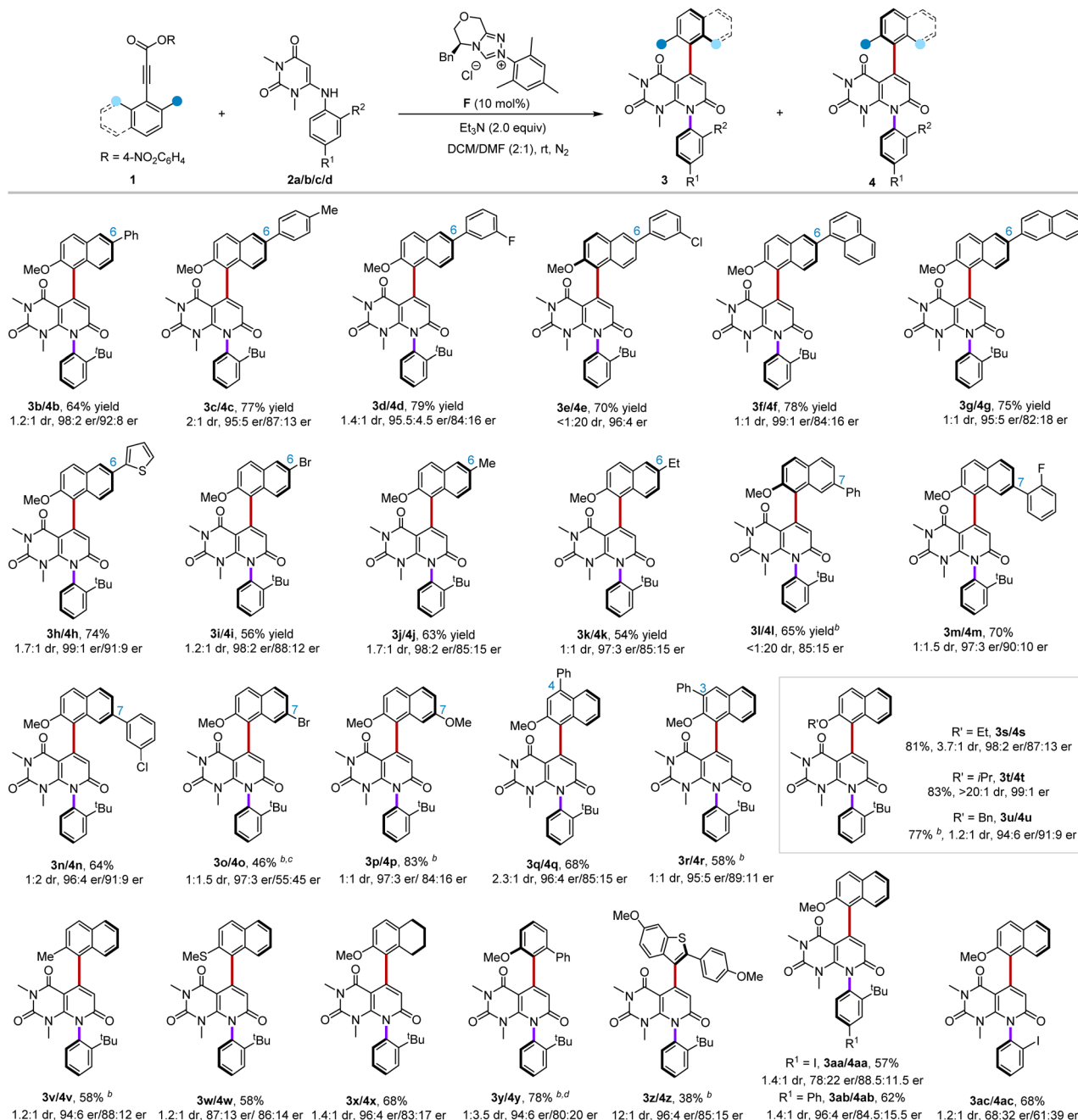
^a **1a** (0.10 mmol, 1.0 equiv.), **2a** (0.12 mmol, 1.2 equiv.), base (0.20 mmol, 2.0 equiv.), precatalyst (0.01 mmol, 10 mol%), 4 ÅMS (25 mg), solvent (2–3 mL), under a N₂ atmosphere. ^b Combined isolated yields based on **1a**. ^c The dr values were determined by ¹H NMR of the crude product. ^d The er values were determined by chiral HPLC analysis. ^e The ratio of volume.

investigated (Scheme 2). Initially, 3-(naphthalene-1-yl) propiolates **1** bearing different substituents at the 6-position were examined. The reactions of alkyne esters **1** bearing 6-aryls, bromo or alkyl groups proceeded smoothly at room temperature to afford the desired products **3b/4b–3d/4d** and **3f/4f–3k/4k** in moderate to good combined yields. Although the diastereoselectivity was not satisfactory for most substrates, diastereomers **3b–d** and **3f–k** were obtained with high to excellent enantioselectivity. Diastereomers **4b–d** and **4f–k** exhibited decreased enantioselectivity compared to model product **4a**. There was an exception that the reaction of 6-(3-chlorophenyl) alkyne ester **1e** produced the diastereomer **4e** in 70% yield with high diastereoselectivity (>20 : 1) and enantioselectivity (96 : 4 er). Then, alkyne esters **1** with diverse 7-substituents were evaluated. It was found that 7-phenyl substituted alkyne ester **1l** yielded the single diastereomer **4l** in 65% yield with 85 : 15 er, while alkyne esters **1m–p** delivered the corresponding products **3m/4m–3p/4p** in moderate to good yields with high enantioselectivity for diastereomer **3m–p**.

It should be noted that the reaction of 7-bromo alkyne ester **1o** did not work under the standard conditions. The employment of NHC-precatalyst **A** could promote the reaction to give

diastereomers **3o/4o** in 46% combined yield with 1 : 1.5 dr, but **4o** was obtained in almost racemic form. Two representative 4-phenyl and 3-phenyl-substituted alkyne esters **1q** and **1r** were also examined. The results were found to be similar to those of the previous substrates with high enantioselectivity for **3q/3r** and moderate enantioselectivity for **4q/4r**. Further replacement of the 2-OMe group of alkyne ester **1a** with 2-OEt (**3s/4s**), 2-OBn (**3u/4u**), 2-Me (**3v/4v**) and 2-SMe (**3w/4w**) resulted in unchanged or slightly decreased enantioselectivities, while replacement of 2-OMe group of **2a** with 2-O*i*Pr (**3t/4t**) led to significantly improved diastereoselectivity (>20 : 1 dr) while maintaining enantioselectivity. Gratifyingly, the reaction of tetrahydronaphthalene alkyne substrate **1x** worked equally well to deliver products with 96 : 4 er for **3x** and 83 : 17 er for **4x**. The reaction of 2-methoxy-6-phenyl-substituted alkyne ester **1y** produced diastereomers **3y** and **4y** in 78% combined yield, with **4y** isolated as the major product with 80 : 20 er. Moreover, a five-membered benzothiophen-3-yl alkyne ester **1z** was used, yielding the desired products **3z/4z** with high diastereoselectivity (12 : 1 dr) and excellent enantioselectivity (97 : 3 er) for the major diastereomer **3z**, albeit with a lower combined yield (38%) due to the low conversion of the substrates. Two





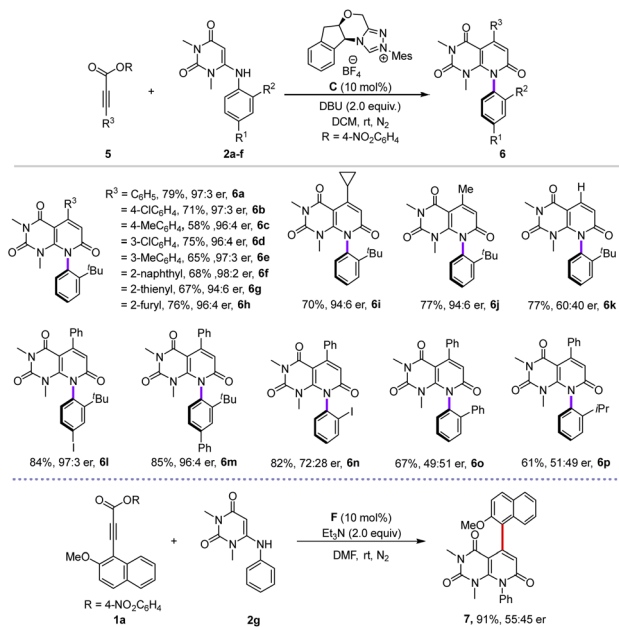
Scheme 2 The reaction scope for the synthesis of fused uracils with C–C and C–N 1,4-diaxes^a. ^aReaction conditions: **1** (0.10 mmol), **2** (0.12 mmol), Et₃N (0.20 mmol), **F** (0.01 mmol), 4 ÅMS (25 mg), anhydrous DCM (2 mL) and DMF (1 mL), under N₂; combined isolated yields based on **1**; the dr values were determined by ¹H NMR of the crude product or HPLC analysis of the isolated products; the er values were determined by chiral HPLC analysis. ^bDMF was used as the solvent, ^cA was used as the NHC pre-catalyst, ^dCS₂CO₃ was used as the base.

representative aminouracils, 6-(2-*tert*-butyl-4-iodophenyl)aminouracil **2b** and 6-(2-*tert*-butyl-4-phenylphenyl)aminouracil **2c**, were also employed to further explore the reaction scope. Interestingly, the reaction with **2b** led to a decrease in enantioselectivity for both diastereomers **3aa** and **4aa**, while the reaction with **2c** maintained enantioselectivity (96 : 4 er) for **3ab** but decreased enantioselectivity (84.5 : 15.5 er) for **4ab**. Last, the effect of the *N*-phenyl *ortho*-group of substrates **2** on the stereoselectivity of this reaction was investigated by replacing the *t*-

butyl group with an iodine group. Unfortunately, this variation led to a significant decrease in the enantioselectivity of both diastereomers **3ac** and **4ac**, which indicated the necessity of an *N*-phenyl *ortho*-group with large steric hindrance.

We then turned our attention to testing the feasibility of constructing fused uracils bearing a single C–N axis.¹⁶ Initially, the reaction conditions for the synthesis of fused uracil **6a** with a single C–N axis were investigated, and the results are included in the ESI (Table S1†). The desired product **6a** was obtained in





Scheme 3 The reaction scope for the synthesis of monoaxial fused uracils^a. ^aReaction conditions: 5 (0.10 mmol), 2 (0.12 mmol), DBU (0.20 mmol), C (0.01 mmol), 4 ÅMS (25 mg), anhydrous DCM (2 mL), under N₂; isolated yields based on 1; the er values were determined by chiral HPLC analysis.

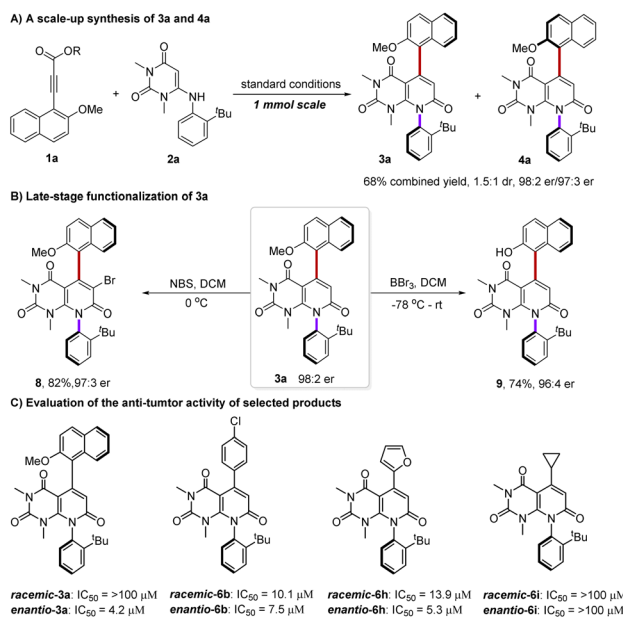


Fig. 1 Synthetic applications and the study of the antitumor activity of selected uracil compounds.

79% yield with 97 : 3 er under the catalysis of precatalyst C using DBU as the base and DCM as the solvent, establishing the optimal conditions for scope exploration (Scheme 3). It was found that the (3 + 3) annulation reaction of aromatic alkyne esters 5 with 6-(2-*tert*-butylphenyl)aminouracil 2a proceeded smoothly to afford the corresponding C–N monoaxial products 6b–h in good yields and with high enantioselectivity.

Gratifyingly, the protocol was also applicable to two representative β -alkyl-substituted aliphatic alkyne esters, and the desired products 6i and 6j were obtained with slightly decreased enantioselectivities. Unfortunately, the reaction of 4-nitrophenyl propiolate gave product 6k in 77% yield with significantly decreased enantioselectivity (60 : 40 er), indicating the significant role of the β -substituents of alkyne esters 5 in the enantio-control process. Then, the influence of substituents on the phenyl ring of 6-phenylaminouracil 2 was studied. For 6-(2-*tert*-butyl-4-iodophenyl)aminouracil 2b and 6-(2-*tert*-butyl-4-phenylphenyl)aminouracil 2c, the desired C–N monoaxial products 6l and 6m were both obtained in high yields and enantioselectivities. However, replacement of the 2-*tert*-butyl group of substrate 2a with smaller groups like iodine (2d), phenyl (2e) and isopropyl (2f) resulted in the formation of product 6n with significantly decreased enantioselectivity and even racemic products 6o and 6p. Moreover, the reaction of 6-phenylaminouracil 2g with 3-(2-methoxynaphthalene-1-yl) propiolate 1a was carried out to examine the possibility of constructing a C–C monoaxial uracil product. Unfortunately, the desired product 7 was obtained in almost racemic form albeit with a high yield. Based on the above results, it can be concluded that the 2-*tert*-butyl group of 6-aminouracils 2 played a crucial role in the enantioselective construction of both monoaxially and 1,4-diaxially chiral uracil products.

To further explore the utility of this protocol, some synthetic applications were then investigated as shown in Fig. 1. First, a 1 mmol scale-up reaction between 1a and 2a under the standard conditions was carried out to afford products 3a and 4a with almost unchanged yields and stereoselectivity (Fig. 1A). Then, late-stage functionalization of product 3a was conducted (Fig. 1B). As a result, bromination and demethylation of 3a delivered products 8 and 9, respectively, in high yields while maintaining enantioselectivity.

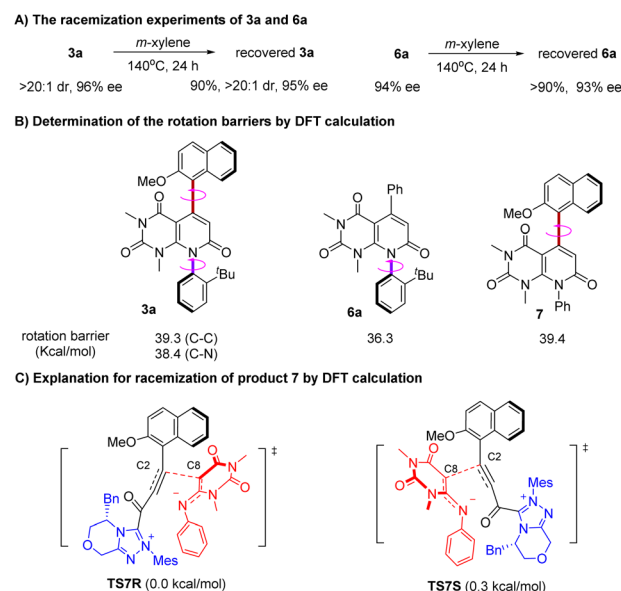


Fig. 2 Determination of the rotational barriers of products 3a/6a/7 and explanation for racemization of 7 through DFT calculations.



To investigate the possible bioactivity of this new class of axially chiral fused uracil scaffolds, the proliferation inhibitory activity of several selected compounds **3a**, **6b**, **6h** and **6i** on MV4-11 human myeloid monocytic leukemia cells was evaluated (Fig. 1C). Among them, enantiopure **3a**, **6b** and **6h** exhibited potent cell proliferation inhibitory activity against MV4-11 cancer cells, with low IC_{50} values ranging from 4.2 to 7.5 μM . In particular, the enantiopure 1,4-biaxially chiral uracil **3a** showed much more potent cell proliferation inhibitory activity ($IC_{50} = 4.2 \mu\text{M}$) than racemic **3a** ($IC_{50} > 100 \mu\text{M}$). Additionally, neither enantiopure nor racemic monoaxially chiral compound **6i** with an alkyl group at the 5-position exhibited cell proliferation inhibitory activity against MV4-11 cancer cells. The above results demonstrated the potential application of this new class of axially chiral uracils as lead compounds for drug discovery.

The thermal stability and rotational barriers of the representative products **3a**, **6a** and **7** were also examined (Fig. 2). The racemization experiments for **3a** and **6a** were conducted in *m*-

xylene at different temperatures (25–140 °C). The results revealed that both diaxially and monoaxially chiral products **3a** and **6a** were stable even at high temperatures because no obvious racemization of **3a** and **6a** was observed at 140 °C for 24 h (Fig. 2A). The experimental results were found to be consistent with the DFT calculated results (Fig. 2B). The rotation barriers for compounds **3a**, **6a** and **7** are higher than 36 kcal mol⁻¹, indicating the high stability of both diaxially and monoaxially chiral products. In order to explain the origin of the formation of racemic product **7**, we further calculated the energy barrier difference between the C2–C8 bond formation transition states, **TS7R** and **TS7S**, involved in the stereo-selectivity-determining step of the reaction. The results shown in Fig. 2C indicate that the energy difference between the two transition states is only 0.3 kcal mol⁻¹, which well explains the racemization of **7** in kinetic terms.

DFT calculations have also been performed to explore the origin of stereoselectivity in the synthesis of 1,4-diaxially chiral

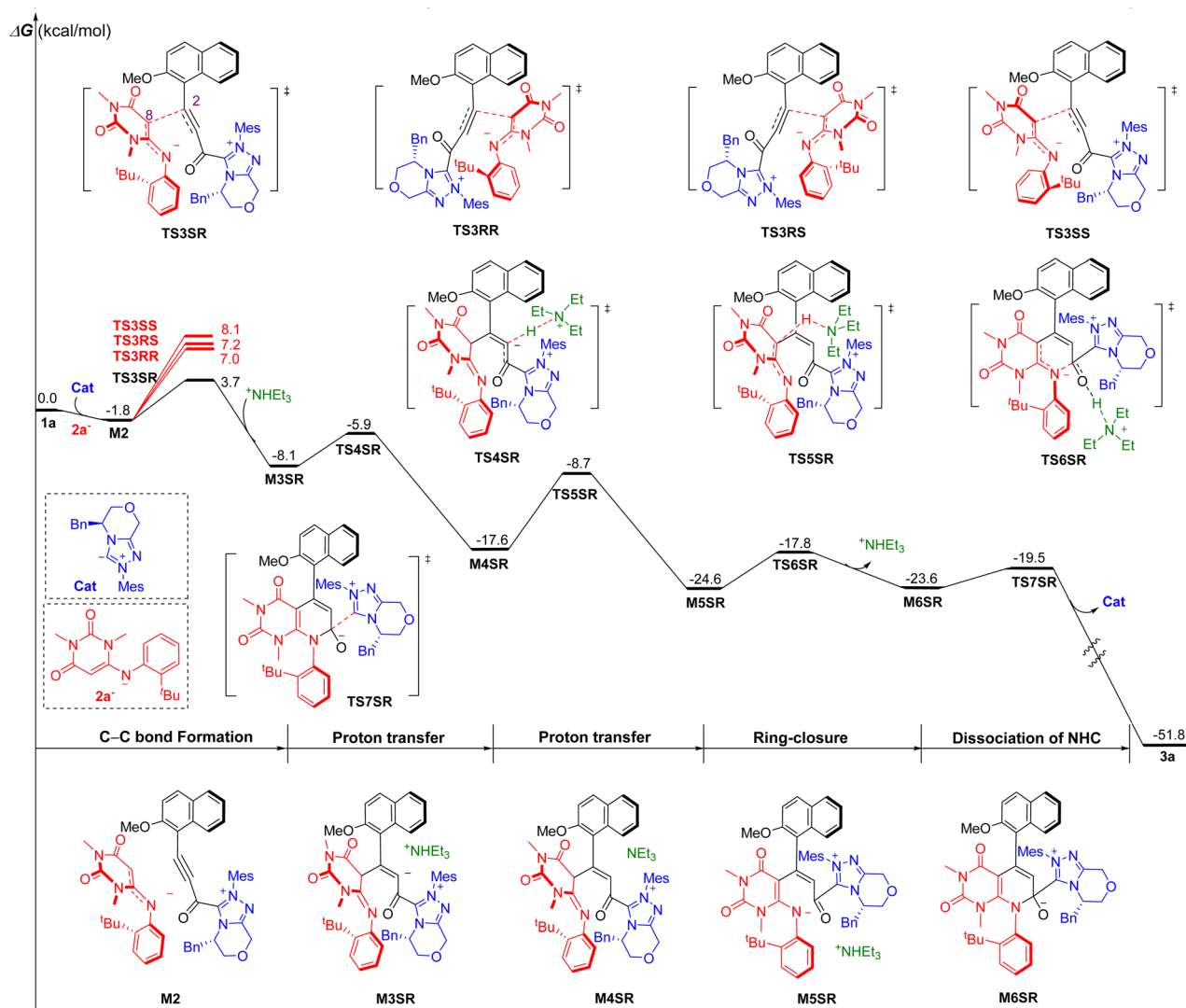


Fig. 3 Relative Gibbs free energy profiles of the reaction. The DFT calculations were performed using the Gaussian 16 program. All structures were optimized by using the M062X functional and 6-31G (d, p) basis set in DCM solvent using the integral equation formalism polarizable continuum model (IEF-PCM).



uracil products, as shown in Fig. 3. The whole reaction is initiated by the nucleophilic addition to **1a** by the actual NHC catalyst (denoted as **Cat**) to form the alkynyl acylazolium intermediate. The subsequent conjugate addition between anion **2a**[−] and the alkynyl acylazolium intermediate leads to the formation of the C2–C8 bond *via* four possible transition states **TS3SR**, **TS3RR**, **TS3RS** and **TS3SS**, respectively. The Gibbs free energy barriers of **TS3SR**, **TS3RR**, **TS3RS** and **TS3SS** are 5.5, 8.8, 9.0 and 9.9 kcal mol^{−1}, respectively, indicating that the SR-configurational pathway is the most energetically favorable pathway. Meanwhile, the smaller energy barrier difference between the above diastereomeric transition states may account for the lower diastereoselectivity of this reaction. Then, only the favorable pathway associated with intermediate **M3SR** has been discussed in the following part. The intermediate **M3SR** transforms to intermediate **M5SR** through a stepwise [1,3]-proton shift through transition states **TS4SR** ($\Delta G^\ddagger = 2.2$ kcal mol^{−1}) and **TS5SR** ($\Delta G^\ddagger = 8.9$ kcal mol^{−1}). The intramolecular nucleophilic addition was responsible for the C–N bond formation *via* transition state **TS6SR** ($\Delta G^\ddagger = 6.8$ kcal mol^{−1}), forming intermediate **M6SR**. At the final step, the free energy barrier for the dissociation of NHC from product **3a** is 4.1 kcal mol^{−1} *via* transition state **TS7SR**. For a detailed description of the reaction process and calculation methods, refer to the ESI.†

Conclusions

In summary, we have demonstrated the first organocatalytic enantioselective synthesis of a new class of fused uracil scaffolds with C–C and C–N 1,4-diaxes *via* NHC-catalyzed atroposelective (3 + 3) annulations of 2,6-disubstituted alkyne esters with 6-aminouracils. This new strategy features a single-step *de novo* pyrido[2,3-*d*]pyrimidine-ring formation accompanied by the simultaneous construction of two different 1,4-diaxes. Moreover, the strategy could be applied to construct C–N monoaxially chiral fused uracil atropisomers in an enantioselective manner. DFT calculations were also performed to explain the origin of the stereoselectivity of this reaction. More importantly, the preliminary study on the anti-tumour activity of selected compounds indicated the potential application of this new class of axially chiral uracils in medicinal chemistry.

Data availability

The data supporting this article have been included as part of the ESI.†

Author contributions

D. D. conceived and designed the study. Y. R., C. L. and Z. L. performed the synthetic experiments. H. Z. and D. W. performed the DFT calculations. J. F. performed the antitumor activity assay.

Conflicts of interest

There are no conflicts to declare.

Acknowledgements

We thank the National Natural Science Foundation of China (No. 22371297) for financial support.

Notes and references

- (a) Z. Wang, L. Meng, X. Liu, L. Zhang, Z. Yu and G. Wu, *Eur. J. Med. Chem.*, 2022, **243**, 114700; (b) A.-C. C. Carlsson, S. Karlsson, R. H. Munday and M. R. Tatton, *Acc. Chem. Res.*, 2022, **55**, 2938–2948; (c) J. K. Cheng, S. H. Xiang, S. Li, L. Ye and B. Tan, *Chem. Rev.*, 2021, **121**, 4805–4902; (d) B. K. Lombe, D. Feineis and G. Bringmann, *Nat. Prod. Rep.*, 2019, **36**, 1513–1545; (e) S. T. Toenjes and J. L. Gustafson, *Future Med. Chem.*, 2018, **10**, 409–422; (f) J. E. Smyth, N. M. Butler and P. A. Keller, *Nat. Prod. Rep.*, 2015, **32**, 1562–1583; (g) A. Zask, J. Murphy and G. A. Ellestad, *Chirality*, 2013, **25**, 265–274; (h) S. R. Laplante, D. F. L. K. R. Fandrick, D. R. Fandrick, O. Hucke, R. Kemper, S. P. Miller and P. J. Edwards, *J. Med. Chem.*, 2011, **54**, 7005–7022; (i) S. R. LaPlante, P. J. Edwards, L. D. Fader, A. Jakalian and O. Hucke, *ChemMedChem*, 2011, **6**, 505–513.
- (a) S. H. Xiang, W. Y. Ding, Y. B. Wang and B. Tan, *Nat. Catal.*, 2024, **7**, 483–498; (b) Z.-H. Li, Q.-Z. Li, H.-Y. Bai and S.-Y. Zhang, *Chem Catal.*, 2023, **3**, 100594; (c) Z. Zhang and L. Dai, *Chem. Sci.*, 2024, **15**, 12636–12643; (d) J. Feng, C.-J. Lu and R.-R. Liu, *Acc. Chem. Res.*, 2023, **56**, 2537–2554; (e) G. Centonze, C. Portolani, P. Righi and G. Bencivenni, *Angew. Chem., Int. Ed.*, 2023, **62**, e202303966; (f) H. H. Zhang and F. Shi, *Acc. Chem. Res.*, 2022, **55**, 2562–2580; (g) P. Rodríguez-Salamanca, R. Fernández, V. Hornillos and J. M. Lassaletta, *Chem.–Eur. J.*, 2022, **28**, e202104442; (h) W. Qin, Y. Liu and H. Yan, *Acc. Chem. Res.*, 2022, **55**, 2780–2795; (i) J. K. Cheng, S.-H. Xiang and B. Tan, *Acc. Chem. Res.*, 2022, **55**, 2920–2937; (j) Y. B. Wang and B. Tan, *Acc. Chem. Res.*, 2018, **51**, 534–547.
- (a) X. Bao, J. Rodríguez and D. Bonne, *Angew. Chem., Int. Ed.*, 2020, **59**, 12623–12634; (b) X. Hu, Y. Zhao, T. He, C. Niu, F. Liu, W. Jia, Y. Mu, X. Li and Z.-Q. Rong, *Chem. Sci.*, 2024, **15**, 13541–13549; (c) T.-J. Han, Q.-L. Yang, J. Hu, M.-C. Wang and G.-J. Mei, *JACS Au*, 2024, **4**, 4445–4454; (d) Y. Wang, X. Zhu, D. Pan, J. Jing, F. Wang, R. Mi, G. Huang and X. Li, *Nat. Commun.*, 2023, **14**, 4661; (e) X.-L. Zhang, J. Gu, W.-H. Cui, Z. Ye, W. Yi, Q. Zhang and Y. He, *Angew. Chem., Int. Ed.*, 2022, **61**, e202210456; (f) B. J. Wang, G. X. Xu, Z. W. Huang, X. Wu, X. Hong, Q. J. Yao and B. F. Shi, *Angew. Chem., Int. Ed.*, 2022, **61**, e202208912; (g) D. Moser and C. Sparr, *Angew. Chem., Int. Ed.*, 2022, **61**, e202202548; (h) Q. Gao, C. Wu, S. Deng, L. Li, Z. S. Liu, Y. Hua, J. Ye, C. Liu, H. G. Cheng, H. Cong, Y. Jiao and Q. Zhou, *J. Am. Chem. Soc.*, 2021, **143**, 7253–7260.
- T. Hayashi, K. Hayashizaki and Y. Ito, *Tetrahedron Lett.*, 1989, **30**, 215–218.
- D. Shen, Y. Xu and S.-L. Shi, *J. Am. Chem. Soc.*, 2019, **141**, 14938–14945.
- (a) T. Shibata, T. Fujimoto, K. Yokota and K. Takagi, *J. Am. Chem. Soc.*, 2004, **126**, 8382–8383; (b) T. Shibata and



- K. Tsuchikama, *Chem. Commun.*, 2005, 6017–6019; (c) T. Shibata, Y. Arai, K. Takami, K. Tsuchikama, T. Fujimoto, S. Takebayashi and K. Takagi, *Adv. Synth. Catal.*, 2006, **348**, 2475–2483.
- 7 K. Tanaka, T. Suda, K. Noguchi and M. Hirano, *J. Org. Chem.*, 2007, **72**, 2243–2246.
- 8 H. Takano, N. Shiozawa, Y. Imai, K. S. Kanyiva and T. Shibata, *J. Am. Chem. Soc.*, 2020, **142**, 4714–4722.
- 9 S. Li, D. Xu, F. Hu, D. Li, W. Qin and H. Yan, *Org. Lett.*, 2018, **20**, 7665–7669.
- 10 O. M. Beleh, E. Miller, F. D. Toste and S. J. Miller, *J. Am. Chem. Soc.*, 2020, **142**, 16461–16470.
- 11 Y.-B. Du, Q.-T. Lu, Y.-S. Cui, K.-W. Wu, Y. Wang, Y.-Z. Zhang, Z. Zhao, J.-L. Hou and Q. Cai, *Angew. Chem., Int. Ed.*, 2024, e202421060.
- 12 (a) Y. Zhang, H. Cai, X. H. Gan and Z. C. Jin, *Sci. China Chem.*, 2024, **67**, 482–511; (b) G. Zhen, K. Jiang and B. Yin, *ChemCatChem*, 2022, **14**, e202200099; (c) B. Zhang and J. Wang, *Sci. China Chem.*, 2022, **65**, 1691–1703; (d) C. De Risi, A. Brandolese, G. Di Carmine, D. Ragno, A. Massi and O. Bortolini, *Chem.–Eur. J.*, 2022, **29**, e202202467; (e) P. Bellotti, M. Koy, M. N. Hopkinson and F. Glorius, *Nat. Rev. Chem.*, 2021, **5**, 711–725; (f) X. Y. Chen, Z. H. Gao and S. Ye, *Acc. Chem. Res.*, 2020, **53**, 690–702; (g) X. Chen, H. Wang, Z. Jin and Y. R. Chi, *Chin. J. Chem.*, 2020, **38**, 1167–1202; (h) S. Mondal, S. R. Yetra, S. Mukherjee and A. T. Biju, *Acc. Chem. Res.*, 2019, **52**, 425–436; (i) C. Zhang, J. F. Hooper and D. W. Lupton, *ACS Catal.*, 2017, **7**, 2583–2596; (j) D. M. Flanagan, F. Romanov-Michailidis, N. A. White and T. Rovis, *Chem. Rev.*, 2015, **115**, 9307–9387; (k) S. Chakraborty, S. Barik and A. T. Biju, *Chem. Soc. Rev.*, 2025, **54**, 1102–1124.
- 13 (a) J. Wang, C. Zhao and J. Wang, *ACS Catal.*, 2021, **11**, 12520–12531; (b) R. Song, Y. Xie, Z. Jin and Y. R. Chi, *Angew. Chem., Int. Ed.*, 2021, **60**, 26026–26037; (c) J. Feng and D. Du, *Tetrahedron*, 2021, **100**, 132456; (d) C. Song, C. Pang, Y. Deng, H. Cai, X. Gan and Y. R. Chi, *ACS Catal.*, 2024, 6926–6935; (e) K. Balanna, S. Barik, S. Barik, S. Shee, N. Manoj, R. G. Gonnade and A. T. Biju, *ACS Catal.*, 2023, **13**, 8752–8759; (f) J.-L. Yan, R. Maiti, S.-C. Ren, W. Tian, T. Li, J. Xu, B. Mondal, Z. Jin and Y. R. Chi, *Nat. Commun.*, 2022, **13**, 84; (g) S.-J. Wang, X. Wang, X. Xin, S. Zhang, H. Yang, M. W. Wong and S. Lu, *Nat. Commun.*, 2024, **15**, 518; (h) Y. Cai, Y. Zhao, K. Tang, H. Zhang, X. Mo, J. Chen and Y. Huang, *Nat. Commun.*, 2024, **15**, 496; (i) S. Barik, S. S. Ranganathappa and A. T. Biju, *Nat. Commun.*, 2024, **15**, 5755; (j) B.-A. Zhou, X.-N. Li, C.-L. Zhang, Z.-X. Wang and S. Ye, *Angew. Chem., Int. Ed.*, 2023, **62**, e202314228; (k) X. Yang, L. Wei, Y. Wu, L. Zhou, X. Zhang and Y. R. Chi, *Angew. Chem., Int. Ed.*, 2023, **62**, e202211977; (l) S. Shee, S. S. Ranganathappa, M. S. Gadhave, R. Gogoi and A. T. Biju, *Angew. Chem., Int. Ed.*, 2023, **62**, e202311709; (m) S. S. Ranganathappa, B. S. Dehury, G. K. Singh, S. Shee and A. T. Biju, *ACS Catal.*, 2024, 6965–6972.
- 14 (a) S. Zhang, X. Wang, L. L. Han, J. Li, Z. Liang, D. Wei and D. Du, *Angew. Chem., Int. Ed.*, 2022, **61**, e202212005; (b) S.-C. Zhang, S. Liu, X. Wang, S.-J. Wang, H. Yang, L. Li, B. Yang, M. W. Wong, Y. Zhao and S. Lu, *ACS Catal.*, 2023, **13**, 2565–2575.
- 15 (a) Z. Dong, C. Jiang and C. Zhao, *Molecules*, 2022, **27**, 7990; (b) J. Gao, S. Zhang and D. Du, *Chem. Rec.*, 2023, **23**, e202300046.
- 16 For NHC-catalyzed construction of C–N monoaxially chiral molecules, see: (a) Y. Chu, M. Wu, F. Hu, P. Zhou, Z. Cao and X. P. Hui, *Org. Lett.*, 2022, **24**, 3884–3889; (b) S. Barik, R. C. Das, K. Balanna and A. T. Biju, *Org. Lett.*, 2022, **24**, 5456–5461; (c) Y. Li, X.-Y. Duan, Y. Wei, J. Li, X. Ren and J. Qi, *Asian J. Org. Chem.*, 2022, **11**, e202200383.

